THE JOURNAL OF BIOLOGICAL CHEMISTRY VOL. 291, NO. 46, pp. 24314–24323, November 11, 2016
Published in the U.S.A.

Impact of Ribonucleotide Backbone on Translesion Synthesis and Repair of 7,8-Dihydro-8-oxoguanine*

Received for publication, May 25, 2016, and in revised form, August 28, 2016 Published, JBC Papers in Press, September 22, 2016, DOI 10.1074/jbc.M116.738732

Akira Sassa[‡1], Melike Çağlayan[§], Yesenia Rodriguez[§], William A. Beard[§], Samuel H. Wilson[§], Takehiko Nohmi[‡], Masamitsu Honma[‡], and Manabu Yasui[‡2]

From the [‡]Division of Genetics and Mutagenesis, National Institute of Health Sciences, 1-18-1 Kamiyoga, Setagaya-ku, Tokyo 158-8501, Japan and the [§]Genome Integrity and Structural Biology Laboratory, National Institutes of Health, National Institute of Environmental Health Sciences, Research Triangle Park, North Carolina 27709

Edited by Patrick Sung

Numerous ribonucleotides are incorporated into the genome during DNA replication. Oxidized ribonucleotides can also be erroneously incorporated into DNA. Embedded ribonucleotides destabilize the structure of DNA and retard DNA synthesis by DNA polymerases (pols), leading to genomic instability. Mammalian cells possess translesion DNA synthesis (TLS) pols that bypass DNA damage. The mechanism of TLS and repair of oxidized ribonucleotides remains to be elucidated. To address this, we analyzed the miscoding properties of the ribonucleotides riboguanosine (rG) and 7,8-dihydro-8-oxo-riboguanosine (8-oxo-rG) during TLS catalyzed by the human TLS pols κ and η *in vitro*. The primer extension reaction catalyzed by human replicative pol α was strongly blocked by 8-oxo-rG. pol κ inefficiently bypassed rG and 8-oxo-rG compared with dG and 7,8-dihydro-8-oxo-2′-deoxyguanosine (8-oxo-dG), whereas pol η easily bypassed the ribonucleotides. pol α exclusively inserted dAMP opposite 8-oxo-rG. Interestingly, pol κ preferentially inserted dCMP opposite 8-oxo-rG, whereas the insertion of dAMP was favored opposite 8-oxo-dG. In addition, pol η accurately bypassed 8-oxo-rG. Furthermore, we examined the activity of the base excision repair (BER) enzymes 8-oxoguanine DNA glycosylase (OGG1) and apurinic/apyrimidinic endonuclease 1 on the substrates, including rG and 8-oxo-rG. Both BER enzymes were completely inactive against 8-oxo-rG in DNA. However, OGG1 suppressed 8-oxo-rG excision by RNase H2, which is involved in the removal of ribonucleotides from DNA. These results suggest that the different sugar backbones between 8-oxo-rG and 8-oxo-dG alter the capacity of TLS and repair of 8-oxoguanine.

DNA replication is essential to maintain genomic integrity. Replicative DNA polymerases (pols)[3] synthesize a new DNA strand by incorporating deoxyribonucleotide triphosphates (dNTPs) with high fidelity. In the cellular nucleotide pool, the concentration of RNA precursors, *i.e.* ribonucleotide triphosphates (rNTPs), is 1 or 2 orders of magnitude higher than that of dNTPs (1, 2). Although pols can discriminate between dNTPs and rNTPs during DNA replication, this selectivity is not perfect (1). More than 10^6 ribonucleotides can be incorporated into the genome per cell (3). Ribonucleotides embedded in the genome are repaired by RNase H2-dependent ribonucleotide excision repair (RER) (4). If ribonucleotides are not efficiently removed from DNA, nucleophilic attack of the 2′-oxygen on the ribonucleotide sugar backbone renders DNA chemically unstable, leading to genomic instability. The absence of RER results in S-phase checkpoint activation (5), slow cell growth (6), and deletion mutations in repetitive DNA sequences in yeast (7). RNase H2 defects are embryonically lethal in mice (3). In humans, mutations in the gene coding RNase H2 are associated with Aicardi-Goutières syndrome, which is a neurological disease with symptoms of systemic autoimmunity (8). The aberrant accumulation of ribonucleotides has been observed in fibroblast cells from RNase H2-defective Aicardi-Goutières syndrome patients (9). Furthermore, the accumulated ribonucleotides activate DNA damage signaling (9), suggesting that ribonucleotide incorporation in DNA could be detrimental to genome stability.

Nucleotides are subjected to oxidation by reactive oxygen species (ROS), which are generated by normal aerobic metabolism in cells (10, 11). 7,8-Dihydro-8-oxo-2′-deoxyguanosine triphosphate (8-oxo-dGTP) is a major oxidized form of dGTP and can be incorporated into the nascent DNA strand during DNA replication and repair (12). 8-Oxo-dG adopts an *anti*-conformation that forms Watson-Crick pairs with cytosine and a *syn*-conformation that forms Hoogsteen pairs with adenine. This causes G to T transversion mutations after DNA replication. Base excision repair (BER) is the primary

* This work was supported by Grant-in-Aid for Young Scientists B (16K16195) and for Scientific Research B (25281022) from the Ministry of Education, Culture, Sports, Science and Technology in Japan and the Intramural Research Program of the National Institutes of Health, NIEHS Grants Z01 ES050158 and Z01 ES050159. The authors declare that they have no conflicts of interest with the contents of this article. The content is solely the responsibility of the authors and does not necessarily represent the official views of the National Institutes of Health.

[1] To whom correspondence may be addressed. Japan. Tel.: 81-3-3700-1141; Fax: 81-3-3700–2348; E-mail: a-sassa@nihs.go.jp.

[2] To whom correspondence may be addressed. Tel.: 81-3-3700-1141; Fax: 81-3-3700-2348; E-mail: m-yasui@nihs.go.jp.

[3] The abbreviations used are: pol, DNA polymerase; RER, ribonucleotide excision repair; 8-oxo-dG, 7,8-dihydro-8-oxo-2′-deoxyguanosine; 8-oxo-rG, 7,8-dihydro-8-oxo-riboguanosine; BER, base excision repair; OGG1, 8-oxoguanine DNA glycosylase; APE1, apurinic/apyrimidinic endonuclease 1; MYH, *MutY* homologue; TLS, translesion DNA synthesis; 6-FAM, 6-carboxyfluorescein; F_{ins}, frequency of insertion; F_{ext}, frequency of extension; ROS, reactive oxygen species.

repair pathway that prevents mutations. In mammalian cells, 8-oxo-dG paired with cytosine is repaired by 8-oxoguanine DNA glycosylase (OGG1)-initiated BER (13). In addition, the *MutY* homologue (MYH) removes an adenine from the 8-oxo-dG:dA mispair (14). Deficiencies in these BER machineries increase G to T transversion mutations, contributing to tumorigenesis (15).

7,8-Dihydro-8-oxo-riboguanosine triphosphate (8-oxo-rGTP), the oxidized rGTP, is also produced by the action of ROS and is known to be detrimental. For example, the addition of 8-oxo-rGTP to a transcription reaction reduces the amount of mRNA and induces mutations in the RNA (16). 8-Oxo-rG in mRNA also retards ribosomal translation (17). Recent studies have shown that 8-oxo-rGTP is incorporated into DNA during replication by *Schizosaccharomyces pombe* pol 4, *Mycobacterium smegmatis* DinB2, and human pol β (18–20), which indicates that 8-oxo-rG exists in the genome.

DNA damages that escape from repair can block replication, possibly leading to cell death. To counteract the deleterious effects of DNA damage, cells possess specialized pols that bypass DNA damage during replication. This process is called translesion DNA synthesis (TLS) and contributes to cell survival by incorporating dNMPs opposite the DNA damage in the template DNA. For example, pol κ incorporates dCMP opposite N^2-guanine adducts of benzo[*a*]pyrene diolepoxide (21–23). pol η accurately and efficiently incorporates nucleotides opposite UV-induced cyclobutane pyrimidine dimers (24, 25). In addition, pols κ and η are involved in error-prone and error-free TLS, respectively, of 8-oxo-dG *in vivo*; pol κ knockdown reduces G to T transversion mutations caused by 8-oxo-dG in human cells (26), and the absence of pol η decreases the accuracy of TLS across 8-oxo-dG in yeast (27).

As with various DNA damages, ribonucleotides in DNA templates retard DNA synthesis *in vitro* by replicative pols δ and ϵ but not by TLS pol ζ (1, 28, 29). Thus, TLS pols are important for the damage tolerance of embedded ribonucleotides. However, it is still unclear whether TLS pols other than pol ζ bypass ribonucleotides. In addition, the miscoding properties of damaged ribonucleotides such as 8-oxo-rG during TLS remain unclear. In this study, we analyzed TLS of rG or 8-oxo-rG by human replicative pol α and TLS pols κ and η as undamaged or damaged ribonucleotide in the template DNA. We observed that pol α efficiently bypassed rG but not 8-oxo-rG. The primer extension reactions catalyzed by pol κ were strongly retarded by rG and 8-oxo-rG. On the other hand, pol η rapidly bypassed rG and 8-oxo-rG as efficiently as dG and 8-oxo-dG. pol α exclusively inserted dAMP opposite 8-oxo-rG and 8-oxo-dG. Both TLS pols κ and η preferentially inserted the correct dCMP opposite 8-oxo-rG, whereas pols were more prone to incorporate dAMP opposite 8-oxo-dG. We also examined the repair of 8-oxo-rG in DNA by BER *in vitro*; OGG1-mediated BER was completely inhibited by the ribonucleotide sugar of 8-oxo-rG. Furthermore, OGG1 interfered with the excision of 8-oxo-rG by RNase H2. Therefore, the ribonucleotide sugar backbone can alter the specificity of TLS and BER activity.

Results

Oxidized Ribonucleotides in DNA Strongly Reduce the Activity of pol α and pol κ but Not pol η—To examine how the structure of ribonucleotide sugar backbones affect TLS catalyzed by pols κ and η, we performed primer extension reactions in the presence of all four dNTPs and varying amounts of pols using unmodified or modified oligonucleotides including rG, 8-oxo-rG, or 8-oxo-dG. Additionally, we also examined the reactions catalyzed by non-TLS pol α. With the unmodified DNA template, all pols rapidly extended primers to form fully extended products (Fig. 1, *A–C, lanes 1–4*). When an 8-oxo-dG-modified template was used for the reaction, pols readily bypassed 8-oxo-dG (Fig. 1, *A–C*, *lanes 13–16*), as previously reported (21, 30, 31). With rG- and 8-oxo-rG-modified templates, rG was found to not retard DNA synthesis by pol α (Fig. 1*A, lanes 5–8*), whereas 8-oxo-rG strongly blocked the extension reaction (Fig. 1*A, lanes 9–12*). The primer extension reactions catalyzed by pol κ were strongly retarded one base before rG and 8-oxo-rG (Fig. 1*B, lanes 5–12*). Increasing amounts of pol κ resulted in bypass across the ribonucleotides to form fully extended products. On the other hand, pol η easily bypassed rG and 8-oxo-rG as efficiently as dG and 8-oxo-dG, respectively (Fig. 1*C*).

Influence of the 8-Oxoguanine Sugar on the Miscoding Specificities Catalyzed by Translesion DNA Polymerases—To examine base substitutions and deletions during TLS, primer extension reactions were performed in the presence of all four dNTPs using pol κ and pol η. The extended products (~28- to 32-mer) past dG, rG, 8-oxo-rG, and 8-oxo-dG were recovered, digested with EcoRI, and subjected to two-phase polyacrylamide gel electrophoresis as described in Fig. 2*A* and under "Experimental Procedures." A standard mixture of six Alexa Fluor 546 (Alexa 546)-labeled oligonucleotides containing dC, dA, dG, or dT opposite the modified nucleotide or one- and two-base deletions can be resolved by this method. The percentage of 2′-deoxynucleotide monophosphate (dNMP) incorporation was normalized to the amount of the starting primer.

When an unmodified or rG-modified substrate was used as the template, pol κ exclusively incorporated dCMP opposite dG and rG (80 ± 2 and 85 ± 3% of the starting primers, respectively) (Fig. 2*B*). Similarly, pol η also incorporated dCMP opposite dG and rG (72 ± 2 and 74 ± 1%, respectively) (Fig. 2*C*). Using an 8-oxo-dG-modified template, pol κ preferentially mis-inserted dAMP (85 ± 4%) opposite 8-oxo-dG followed by slight incorporation of dCMP (9 ± 1%). pol η incorporated dCMP (46 ± 2%) and lesser amounts of dAMP and dGMP (18 ± 1, and 8 ± <1%, respectively). Some unknown products were also observed (*arrowheads* in Fig. 2*C*) as previously reported (32, 33). Using an 8-oxo-rG-modified template, pol κ preferentially incorporated the correct dCMP (47 ± 5%) opposite 8-oxo-rG rather than dAMP (25 ± 3%). 8-Oxo-rG also directed insertion of dCMP (43 ± 4%), dAMP (21 ± 3%), and dGMP (11 ± 2%) catalyzed by pol η.

Steady-state Kinetic Studies on rG-, 8-Oxo-dG-, and 8-Oxo-rG-modified DNA Templates—To more accurately measure the frequency of dNMP incorporation (F_{ins}) opposite rG, 8-oxo-dG, or 8-oxo-rG and chain extension (F_{ext}) from the

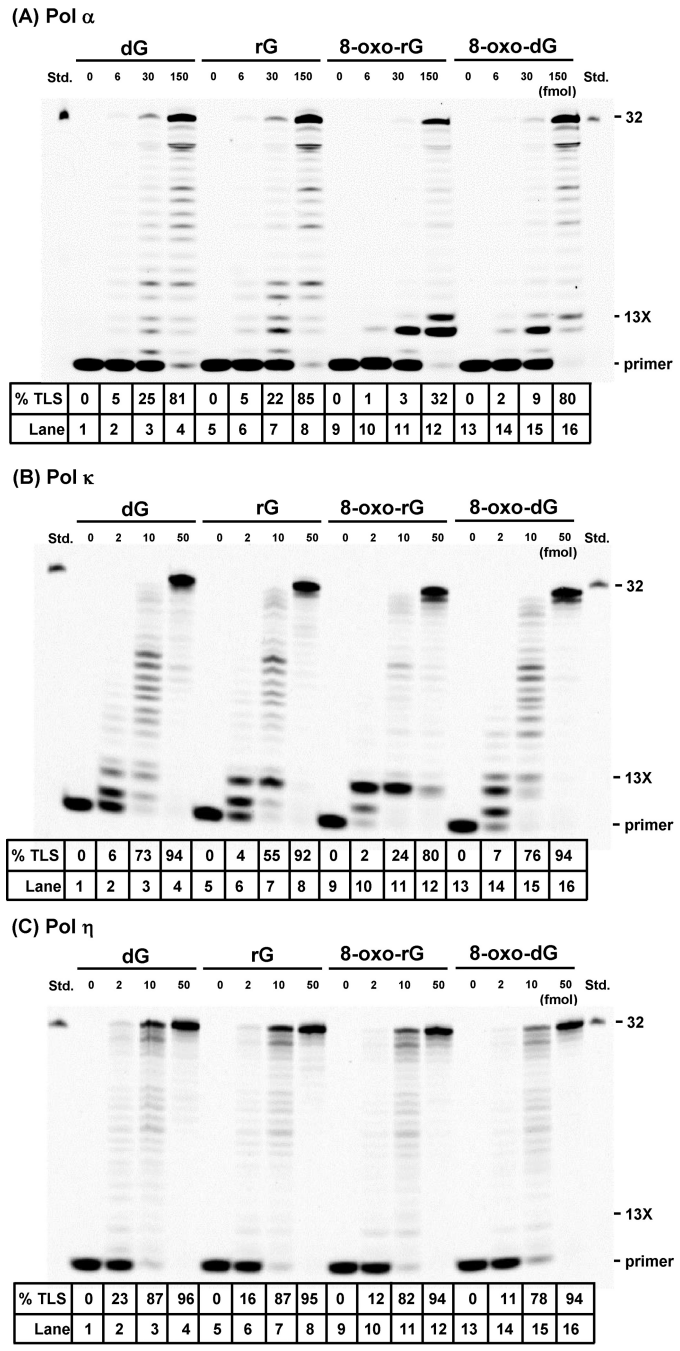

FIGURE 1. **Primer extension reactions catalyzed by DNA polymerases on rG-, 8-oxo-rG, and 8-oxo-dG-modified DNA templates.** Unmodified or modified 38-mer template DNA was annealed to an Alexa 546-labeled 10-mer primer. Reactions catalyzed by varying amounts of human pols α (6, 30, or 150 fmol) (*A*), κ (2, 10, or 50 fmol) (*B*), and η (2, 10, or 50 fmol) (*C*) were performed at 25 °C for 30 min in the presence of dNTPs. *13X* indicates the position of the modification. % *TLS* indicates the percentage of the amount of primers beyond the lesion relative to the total amount of the primer.

primer terminus, steady-state kinetic analysis was performed using pols α, κ, and η.

Regarding pol α (Table 1), the F_{ins} for dCMP incorporation opposite rG (2.98×10^{-1}) was slightly lower than that for dCMP insertion opposite dG. The F_{ext} for dC:rG (2.50×10^{-1}) was also somewhat lower than that for dC:dG, resulting in a relative bypass frequency ($F_{ins} \times F_{ext}$) for dC:rG of 7.44×10^{-2}. The F_{ins} for dCMP incorporation opposite 8-oxo-dG (3.87×10^{-3}) was 3.6-fold lower than that for dAMP incorporation (1.40×10^{-2}). The F_{ext} for dC:8-oxo-dG (7.31×10^{-4}) was 70-fold lower than that for dA:8-oxo-dG (5.14×10^{-2}). Accordingly, the $F_{ins} \times F_{ext}$ for dC:8-oxo-dG was 250-fold lower than that for dA:8-oxo-dG. The $F_{ins} \times F_{ext}$ for dA:8-oxo-rG was 5.33×10^{-5}. $F_{ins} \times F_{ext}$ for dC:8-oxo-rG, dG:8-oxo-rG, and dT:8-oxo-rG were too low to measure accurately.

Next, the F_{ins} and F_{ext} for dG, rG, 8-oxo-dG, or 8-oxo-rG were determined using pol κ (Table 2). The F_{ins} for dCMP incorporation opposite rG (1.08×10^{-2}) was 2 orders of magnitude lower than that for dCMP incorporation opposite dG. The $F_{ins} \times F_{ext}$ for dC:rG was 130-fold lower than that for dC:dG. Comparing the frequency of dCMP and dAMP incorporation opposite 8-oxo-dG, the F_{ins} for dCMP incorporation (7.45×10^{-3}) was 5-fold lower than that for dAMP (3.73×10^{-2}). The F_{ext} for dC:8-oxo-dG (1.77×10^{-2}) was 2-fold lower than that for dA:8-oxo-dG (3.72×10^{-2}). Therefore, the $F_{ins} \times F_{ext}$ for dC:8-oxo-dG was 10-fold lower than that for dA:8-oxo-dG. On the other hand, the F_{ins} for the correct dCMP insertion opposite 8-oxo-rG (6.38×10^{-4}) was 1.4- and 55-fold higher than that for dAMP (4.70×10^{-4}) and dTMP (1.17×10^{-5}), respectively. In addition, the F_{ext} for dC:8-oxo-rG (3.83×10^{-2}) was 1.9- and 14-fold higher than that for dA:8-oxo-rG (2.04×10^{-2}) and dT:8-oxo-rG (2.69×10^{-3}), respectively. This increased the $F_{ins} \times F_{ext}$ for dC:8-oxo-rG 2.5- and 770-fold more than that for dA:8-oxo-rG and dT:8-oxo-rG, respectively. The incorporation efficiency of dGMP opposite 8-oxo-rG was too low to measure accurately.

We also measured the F_{ins} and F_{ext} for the substrates using pol η (Table 3). The F_{ins} for dCMP incorporation opposite rG (4.90×10^{-1}) was 2-fold lower than that for dG. Because the F_{ext} for dC:rG (1.21) was comparable with that for dC:dG, the $F_{ins} \times F_{ext}$ past dC:rG was only 1.7-fold lower than that for dC:dG. The values of F_{ins} for dCMP and dAMP incorporation opposite 8-oxo-dG were similar (2.82×10^{-1} and 3.19×10^{-1}, respectively). The $F_{ins} \times F_{ext}$ past dC:8-oxo-dG and dA:8-oxo-dG were comparable because the F_{ext} values were similar between dC:8-oxo-dG and dA:8-oxo-dG (1.37 and 1.53, respectively). Next, the F_{ins} for the incorporation of the correct nucleotide (dCMP) opposite 8-oxo-rG (2.63×10^{-1}) was 2.7-fold higher than that for dAMP (9.87×10^{-2}) and was 4.9- and 67-fold higher than those for dGMP and dTMP, respectively. The $F_{ins} \times F_{ext}$ for dC:8-oxo-rG was 2.5-fold higher than that for dA:8-oxo-rG and was 53- and 510-fold higher than that for dG:8-oxo-rG and dT:8-oxo-rG, respectively.

Base Excision Repair Is Unable to Repair 8-Oxo-rG—Next, we examined the effect of the ribonucleotide backbone on OGG1 activity in the absence or presence of apurinic/apyrimidinic endonuclease 1 (APE1) using substrates containing rG, 8-oxo-rG, or 8-oxo-dG (Fig. 3). OGG1 and APE1 did not excise rG (Fig. 3, *lanes 2* and *3*), compared with the control reaction that shows complete excision of 8-oxo-dG (Fig. 3, *lanes 8* and *9*). Similarly, OGG1 with or without APE1 was not active against 8-oxo-rG (Fig. 3, *lanes 5* and *6*).

Suppression of RNase H2 Activity by 8-Oxoguanine and OGG1—Our working model suggests that 8-oxo-rG could not be efficiently excised by RNase H2 due to the presence of the abnormal base, *i.e.* 8-oxoguanine. Furthermore, specific bind-

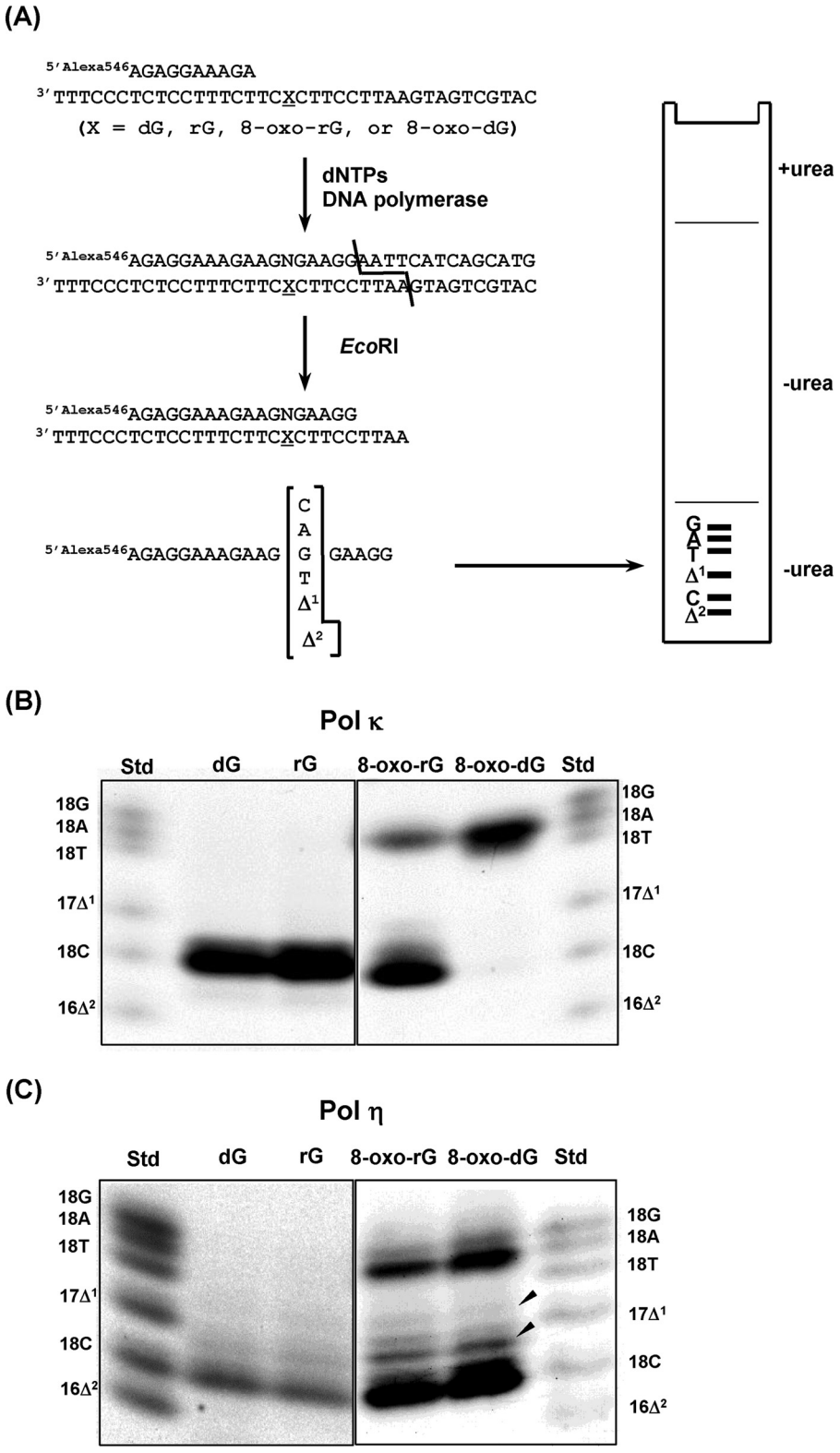

FIGURE 2. **Miscoding specificities of rG, 8-oxo-rG, and 8-oxo-dG during translesion synthesis.** *A,* overview of two-phase PAGE analysis. Unmodified or modified 38-mer template DNA was annealed to an Alexa 546-labeled 10-mer primer. Primer extension reactions catalyzed by 50 fmol of human pol κ (*B*) or pol η (*C*) were performed for 30 min at 25 °C in the presence of dNTPs. The fully extended products were extracted from the polyacrylamide gel. Then, the extracted products were annealed with a complementary 38-mer, digested with EcoRI, and loaded onto a two-phase polyacrylamide gel. To analyze miscoding properties, the mobility of the products were compared with those of Alexa 546-labeled 18-mer standard oligonucleotides containing dC (*18C*), dA (*18A*), dG (*18G*), or dT (*18T*) opposite the lesion and one- (Δ^1) or two-base (Δ^2) deletions. The miscoding properties (%) were quantified and presented as the mean ± S.E. of at least two independent experiments under "Results."

TABLE 1

Kinetic parameters for nucleotide insertion and chain extension reactions catalyzed by human DNA polymerase α

Frequencies of nucleotide insertion (F_{ins}) and chain extension (F_{ext}) were estimated by the following equation: $F = (V_{max}/K_m)_{[wrong\ pair]}/(V_{max}/K_m)_{[correct\ pair\ =\ dC:dG]}$. ND, reliable kinetic parameters could not be determined under steady-state conditions.

	Insertion dNTP			Extension dGTP			
	↓GAAGAAAGGAGA			↓NGAAGAAAGGAGA			
	5'CCTTCXCTTCTTTCCTCTCCCTTT			5'CCTTCXCTTCTTTCCTCTCCCTTT			
N:X	K_m (μM)[a]	k_{cat} (min^{-1})[a]	F_{ins}	K_m (μM)[a]	k_{cat} (min^{-1})[a]	F_{ext}	$F_{ins} \times F_{ext}$
dC:dG	2.07 ± 0.470	0.162 ± 0.0121	1	2.70 ± 0.668	0.226 ± 0.0151	1	1
dC:rG	9.43 ± 1.84	0.220 ± 0.0138	2.98×10^{-1}	8.71 ± 2.05	0.182 ± 0.0135	2.50×10^{-1}	7.44×10^{-2}
dC:8-oxo-rG	3210 ± 767	0.0836 ± 0.0128	3.33×10^{-4}	ND	ND	ND	ND
dA:8-oxo-rG	446 ± 168	0.146 ± 0.0195	4.18×10^{-3}	209 ± 19.4	0.223 ± 0.00740	1.27×10^{-2}	5.33×10^{-5}
dG:8-oxo-rG	ND	ND	ND	ND	ND	ND	ND
dT:8-oxo-rG	ND	ND	ND	ND	ND	ND	ND
dC:8-oxo-dG	390 ± 81.3	0.118 ± 0.0107	3.87×10^{-3}	693 ± 96.4	0.0424 ± 0.00312	7.31×10^{-4}	2.83×10^{-6}
dA:8-oxo-dG	151 ± 24.3	0.166 ± 0.00860	1.40×10^{-2}	38.6 ± 6.73	0.166 ± 0.00984	5.14×10^{-2}	7.21×10^{-4}

[a] Data were expressed as mean ± S.E. obtained from three independent experiments.

TABLE 2

Kinetic parameters for nucleotide insertion and chain extension reactions catalyzed by human DNA polymerase κ

Frequencies of nucleotide insertion (F_{ins}) and chain extension (F_{ext}) were estimated by the following equation: $F = (V_{max}/K_m)_{[wrong\ pair]}/(V_{max}/K_m)_{[correct\ pair\ =\ dC:dG]}$. ND, reliable kinetic parameters could not be determined under steady-state conditions.

	Insertion dNTP			Extension dGTP			
	↓GAAGAAAGGAGA			↓NGAAGAAAGGAGA			
	5'CCTTCXCTTCTTTCCTCTCCCTTT			5'CCTTCXCTTCTTTCCTCTCCCTTT			
N:X	K_m (μM)[a]	k_{cat} (min^{-1})[a]	F_{ins}	K_m (μM)[a]	k_{cat} (min^{-1})[a]	F_{ext}	$F_{ins} \times F_{ext}$
dC:dG	2.10 ± 0.776	27.4 ± 5.73	1	1.1 ± 0.176	13.3 ± 0.986	1	1
dC:rG	141 ± 39.4	19.8 ± 2.77	1.08×10^{-2}	1.55 ± 0.455	13.4 ± 1.28	7.15×10^{-1}	7.70×10^{-3}
dC:8-oxo-rG	3750 ± 895	31.2 ± 4.98	6.38×10^{-4}	29.6 ± 3.65	13.7 ± 0.671	3.83×10^{-2}	2.44×10^{-5}
dA:8-oxo-rG	1050 ± 210	6.44 ± 0.776	4.70×10^{-4}	51.9 ± 5.58	12.8 ± 0.512	2.04×10^{-2}	9.59×10^{-6}
dG:8-oxo-rG	ND	ND	ND	362 ± 61.0	1.11 ± 0.0794	2.54×10^{-4}	ND
dT:8-oxo-rG	1430 ± 294	0.219 ± 0.0227	1.17×10^{-5}	246 ± 33.7	8.00 ± 0.410	2.69×10^{-3}	3.16×10^{-8}
dC:8-oxo-dG	221 ± 45.8	21.5 ± 1.61	7.45×10^{-3}	58.1 ± 8.64	12.4 ± 0.567	1.77×10^{-2}	1.32×10^{-4}
dA:8-oxo-dG	16.7 ± 1.99	8.14 ± 0.262	3.73×10^{-2}	26.0 ± 3.53	11.7 ± 0.603	3.72×10^{-2}	1.39×10^{-3}

[a] Data were expressed as mean ± S.E. obtained from three independent experiments.

ing of OGG1 to 8-oxoguanine-containing DNA (34) may influence the RNase-mediated cleavage of 8-oxo-rG, because DNA glycosylases bound to the damaged base could inhibit damage processing by other enzymes (20, 35, 36). To investigate this model, the activity of RNase H2 was compared in the absence or presence of OGG1 for different substrates including rG or 8-oxo-rG (Fig. 4, *A* and *B*). We observed complete cleavage of rG by RNase H2 (Fig. 4*A*, *lanes 2–4*), which was not affected by the addition of OGG1 (Fig. 4*A*, *lanes 5–7*). With the 8-oxo-rG substrate, the activity of RNase H2 was decreased (Fig. 4*A*, *lanes 9–11*), and 8-oxo-rG excision was further suppressed in the presence of OGG1 (Fig. 4*A*, *lanes 12–14*). Quantification of the results indicate that RNase H2 was inhibited ~4-fold by OGG1 (Fig. 4*B*). Furthermore, the binding capacity of OGG1 was analyzed and compared for the substrates with 8-oxo-dG and 8-oxo-rG. The results showed that OGG1 was capable of binding to 8-oxo-rG (Fig. 4*C*), which could interfere with RNase H2 (Fig. 4*A*).

Discussion

The concentration of rGTP (~500 μM) is 2 orders of magnitude higher than that of dGTP (~5 μM) in cells (2), implying that a substantial amount of 8-oxo-rGTP can be produced in the presence of ROS. Because rNTPs (including 8-oxo-rGTP) can be incorporated into DNA during replication, ribonucleotides, if not repaired, are problematic DNA lesions due to its potential to retard DNA replication (1, 28). However, the ability of pols α, κ, and η to bypass the ribonucleotides is still unclear. Furthermore, little is known about the repair mechanisms of oxidized ribonucleotides such as 8-oxo-rG. In this study, we analyzed the activities and specificities of TLS across rG or 8-oxo-rG catalyzed by pols α, κ, and η. In addition, the

TABLE 3

Kinetic parameters for nucleotide insertion and chain extension reactions catalyzed by human DNA polymerase η

Frequencies of nucleotide insertion (F_{ins}) and chain extension (F_{ext}) were estimated by the following equation: $F = (V_{max}/K_m)_{[wrong\ pair]}/(V_{max}/K_m)_{[correct\ pair\ =\ dC:dG]}$. ND, reliable kinetic parameters could not be determined under steady-state conditions.

	Insertion dNTP			Extension dGTP			
	↓GAAGAAAGGAGA			↓NGAAGAAAGGAGA			
	5′CCTTCXCTTCTTTCCTCTCCCTTT			5′CCTTCXCTTCTTTCCTCTCCCTTT			
N:X	K_m (μM)[a]	k_{cat} (min^{-1})[a]	F_{ins}	K_m (μM)[a]	k_{cat} (min^{-1})[a]	F_{ext}	$F_{ins} \times F_{ext}$
dC:dG	1.07 ± 0.103	2.11 ± 0.0605	1	0.283 ± 0.0795	1.25 ± 0.0955	1	1
dC:rG	3.24 ± 1.13	3.13 ± 0.334	4.90×10^{-1}	0.276 ± 0.0520	1.48 ± 0.0700	1.21	5.95×10^{-1}
dC:8-oxo-rG	2.45 ± 0.0485	1.27 ± 0.0740	2.63×10^{-1}	0.275 ± 0.0568	0.730 ± 0.0363	6.01×10^{-1}	1.58×10^{-1}
dA:8-oxo-rG	4.24 ± 1.86	0.825 ± 0.118	9.87×10^{-2}	0.234 ± 0.0400	0.650 ± 0.0256	6.29×10^{-1}	6.21×10^{-2}
dG:8-oxo-rG	3.59 ± 0.421	0.384 ± 0.0122	5.42×10^{-2}	1.40 ± 0.256	0.338 ± 0.0158	5.47×10^{-2}	2.96×10^{-3}
dT:8-oxo-rG	113 ± 24.9	0.88 ± 0.0715	3.95×10^{-3}	1.01 ± 0.355	0.374 ± 0.0307	8.38×10^{-2}	3.31×10^{-4}
dC:8-oxo-dG	2.59 ± 0.559	1.44 ± 0.0930	2.82×10^{-1}	0.233 ± 0.0398	1.41 ± 0.0575	1.37	3.86×10^{-1}
dA:8-oxo-dG	3.27 ± 0.861	2.06 ± 0.176	3.19×10^{-1}	0.161 ± 0.0256	1.09 ± 0.0461	1.53	4.90×10^{-1}

[a] Data were expressed as mean ± S.E. obtained from three independent experiments.

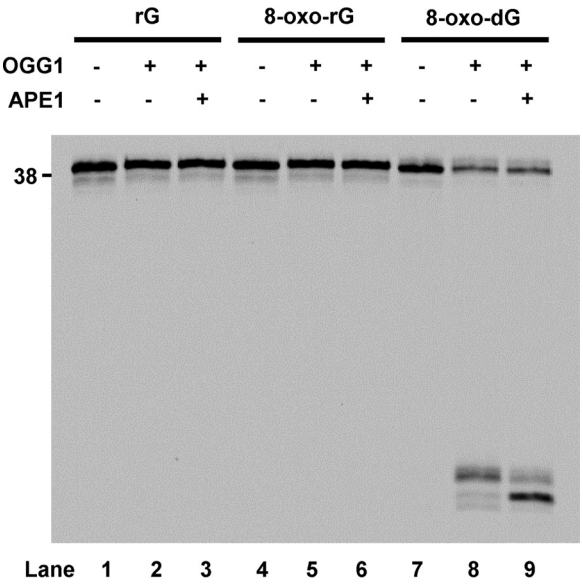

FIGURE 3. **Effect of the ribonucleotide backbone on the BER activity.** The 5′-end 6-FAM-labeled DNA substrate containing rG, 8-oxo-rG, or 8-oxo-dG (200 nM) was incubated for 30 min at 37 °C in the absence (−) or presence (+) of OGG1 (100 nM) and APE1 (40 nM).

influence of the 8-oxo-rG sugar backbone on the activity of BER enzymes was examined.

We found that the replicative pol α efficiently bypassed rG but not 8-oxo-rG. Furthermore, pol α exclusively inserted dAMP opposite 8-oxo-rG. These results suggest that 8-oxo-rG in DNA can be highly cytotoxic and pro-mutagenic. This result highlights the importance of TLS pols for the damage tolerance against the ribonucleotide. Regarding TLS pols, primer extension reactions catalyzed by pol κ were retarded by rG or 8-oxo-rG one base before the ribonucleotide. In contrast, pol η easily bypassed rG and 8-oxo-rG as efficiently as dG and 8-oxo-dG, respectively. This was also supported by steady-state kinetic analyses. The different TLS efficiencies between pol κ and η may reflect the evolution of their active sites to bypass specific DNA template lesions. pol η, but not pol κ, constitutes a molecular splint that stabilizes the structure of damaged DNA (37, 38). This might enable pol η to efficiently bypass the ribonucleotide. Both pols exclusively inserted the correct nucleotide (dCMP) opposite rG, indicating that rG itself does not have a miscoding potential during TLS.

According to our steady-state kinetic analyses, dCMP was preferably inserted opposite 8-oxo-rG when bypassed by pols κ and η; the ratio of dCMP/dAMP insertion for 8-oxo-rG during TLS was 2.5 in the reactions catalyzed by both pol κ and pol η, whereas the ratio for 8-oxo-dG was 0.095 and 0.79 in the reactions by pol κ and pol η, respectively (Tables 2 and 3). Albeit the structural mechanism of 8-oxoguanine bypass is different between human pol κ and pol η (31, 39), the specificities of TLS catalyzed by both TLS pols were influenced by the sugar identity of 8-oxoguanine. Thus, it is plausible that the ribose sugar affects the conformation of the 8-oxoguanine base itself in the active sites of pols κ and η that are more open and flexible than those of replicative pols. At physiological pH, 8-oxoguanine has a carbonyl group at C8 and a proton at N7. Therefore, when 8-oxo-dG is paired with cytosine in the *anti*-conformation, a steric clash could occur between the C8-oxygen of 8-oxoguanine and O4′ of the deoxyribose sugar (40, 41). Comparing the structure of the normal duplex DNA and the DNA containing a single ribonucleotide, the sugar pucker conformation of an embedded ribonucleotide is locally changed to C3′-endo, whereas that of deoxyribonucleotides in the normal DNA is C2′-endo (42). Because the sugar pucker conformation also affects the position of the base (42), sugar puckering of the ribose in 8-oxo-rG might change the position of 8-oxoguanine to avoid a potential steric clash between the C8-oxygen of 8-oxoguanine and the O4′ of the sugar moiety, thereby promoting Watson-Crick pairing with cytosine. Because the active site of pol κ is adapted to accommodate 8-oxoguanine in the *syn*-conformation (39), the structural change of 8-oxoguanine in the *anti*-conformation by the ribose sugar might distort the active

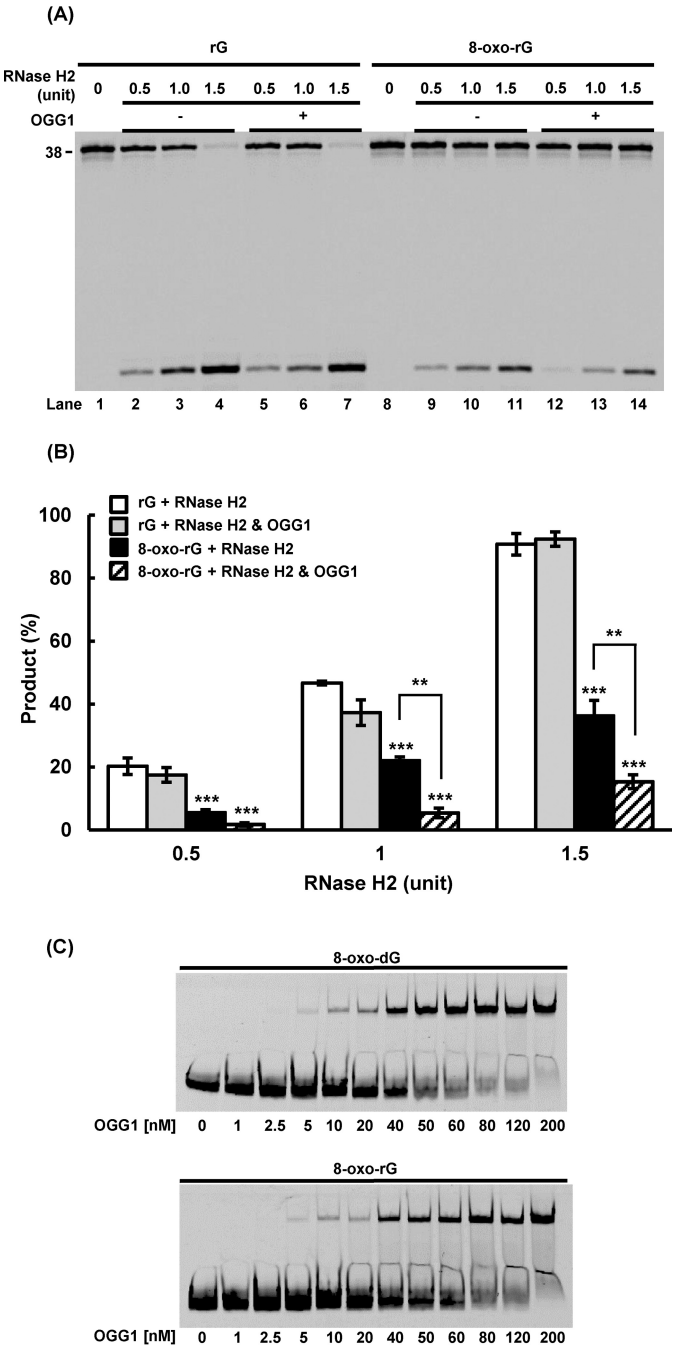

FIGURE 4. **Effect of OGG1 on RNase H2-mediated ribonucleotide excision.** *A*, the 5′-end 6-FAM-labeled DNA substrate containing rG or 8-oxo-rG (200 nM) was incubated with RNase H2 (0.5, 1.0, or 1.5 units) for 60 min at 37 °C in the absence (−) or presence (+) of OGG1 (750 nM). *B*, quantification of the product formed by RNase H2-mediated excision. ***, $p < 0.001$ when compared with "rG + RNase H2." **, $p < 0.01$ between "8-oxo-rG + RNase H2" and "8-oxo-rG + RNase H2 and OGG1." Values presented are the mean ± S.E. of four independent experiments. *C*, gel mobility shift assay to assess the substrate binding capacity of OGG1. The 5′-end 6-FAM-labeled DNA substrate containing 8-oxo-dG or 8-oxo-rG (50 nM) was incubated with varying amounts of OGG1 for 15 min on ice.

site and result in stronger retardation of TLS compared with rG (Table 2).

The ribonucleotide sugar backbone completely inhibited the excision of 8-oxo-rG by OGG1 and APE1, suggesting that the oxidized ribonucleotide was not repaired by BER. These findings suggest the following two possibilities: (i) OGG1 cannot remove 8-oxoguanine from 8-oxo-rG, or (ii) even if OGG1 removes 8-oxoguanine from 8-oxo-rG, the resulting abasic ribonucleotide is resistant to the lyase and AP-endonuclease activities of OGG1 and APE1, respectively. In the first case, the ribonucleotide backbone inhibits the flipping of 8-oxoguanine into the active site of OGG1, which is an essential step in the glycosylase reaction (43). Alternatively, even if base-flipping occurs, nucleophilic attack by the active site residue at the C1′ position of ribose may not occur because of the steric hindrance with the 2′-OH of the ribose. The second scenario implies that the abasic ribonucleotide in DNA might be chemically and enzymatically resistant. Consistent with this idea, it has previously been demonstrated that an abasic RNA is more chemically stable than an abasic DNA (44). Further studies are needed to clarify the biochemical and biological relevance of abasic ribonucleotides in the genome.

Although RNase H2 was able to cleave 8-oxo-rG, it did so with lower efficiency than rG. In addition, OGG1 significantly suppressed 8-oxo-rG cleavage by RNase H2. Similarly, it has previously been shown that MYH cannot remove rA paired with 8-oxo-dG and interferes with the excision of rA by RNase H2 (20). Taken together, BER components have detrimental effects on ribonucleotide repair by RER when ribonucleotides "mimic" BER substrates. Thus, 8-oxo-rG is a poor substrate relative to undamaged ribonucleotides for RNase H2, supporting the idea that TLS pols are crucial for a damaged ribonucleotide tolerance pathway. The repair of 8-oxo-rG in the genome may rely on other repair pathways. The nucleotide excision repair pathway removes helix-distorting adducts and can play significant roles in the repair of ribonucleotides and oxidized DNA damages (45–48). Thus, nucleotide excision repair may be involved in the repair of 8-oxo-rG to stabilize the genome.

In summary, our results suggest that 8-oxo-rG has the strong miscoding potential and acts as a replication blocking lesion for pol α. In contrast, 8-oxo-rG is bypassed by pols κ and η, which preferentially inserts dCMP opposite 8-oxo-rG. BER cannot remove 8-oxo-rG and suppresses its excision by RNase H2. Based on these findings, we concluded that the sugar of the damaged nucleotide alters the capacity and specificity of TLS and repair *in vitro*. It would be interesting to examine the mutagenic potential and repair mechanisms of 8-oxo-rG in cells. Further investigation is required to completely understand the cellular impact of damaged ribonucleotides.

Experimental Procedures

Materials—Ultrapure dNTPs were purchased from GE Healthcare. Unmodified DNA templates, Alexa 546-labeled primers, and standard markers were purchased from Japan Bio Service (Saitama, Japan). Alexa 546 was conjugated to the 5′-terminus of primers and standard markers. DNA templates containing rG, 8-oxo-rG, and 8-oxo-dG were synthesized by Tsukuba Oligo Service Co., Ltd. (Ibaraki, Japan). 5′-End 6-carboxyfluorescein (6-FAM)-labeled oligonucleotides were obtained from Integrated DNA Technologies Inc. (IL). Human pol α was purchased from CHIMERx (WI). Human pol κ was purified as C-terminal truncations with 10 His tags as previously described (49). Human pol η was purchased from Enzy-

max (KY). Human OGG1 and APE1 were purified as previously described (50, 51). RNase H2 was purchased from New England Biolabs (MA).

Primer Extension Reactions—Primer extension assays were performed at 25 °C for 30 min in reaction buffer (10 μl) containing all four dNTPs (100 μM each) using unmodified or 8-oxo-dG-, 8-oxo-rG-, or rG-modified 38-mer templates (750 fmol) primed with an Alexa 546-labeled 10-mer primer (500 fmol, 5′-AGAGGAAAGA). The reaction buffer for pols κ and η contained 40 mM Tris-HCl (pH 8.0), 5 mM $MgCl_2$, 10 mM dithiothreitol, 250 μg/ml of BSA, 60 mM KCl, and 2.5% glycerol. Reactions were initiated by the addition of enzyme. Reactions were terminated by incubating in 10 μl of formamide dye containing blue dextran (25 mg/ml) and EDTA (10 mM) at 95 °C for 3 min. The reaction samples (10 μl) were subjected to 20% denaturing PAGE (30 × 40 × 0.05 cm). The separated products were visualized using Molecular Imager FX Pro and Quantity One software (Bio-Rad Laboratories) or Typhoon PhosphorImager and ImageQuant software (GE Healthcare).

Observation of Miscoding Specificities and Frequencies—Primer extension reactions were conducted at 25 °C for 30 min by adding 50 fmol of pol κ or pol η in a buffer (10 μl) containing all four dNTPs (100 μM each) and 38-mer templates (750 fmol) primed with an Alexa 546-labeled 10-mer primer (500 fmol, 5′-AGAGGAAAGA). The fully extended products were extracted from the gel. The recovered oligonucleotides were annealed with the unmodified 38-mer, cleaved with EcoRI, and subjected to two-phase PAGE (20 × 65 × 0.05 cm) containing 7 M urea in the upper phase and no urea in the middle and bottom phases. The phase width was 10, 37, and 18 cm for the upper, middle, and bottom phases, respectively. To quantify base substitutions and deletions, the mobility of the reaction products was compared with those of Alexa 546-labeled 18-mer standard markers containing dC, dA, dG, or dT opposite the lesion and one-base (Δ^1) or two-base (Δ^2) deletions (Fig. 2*A*) (33, 52).

Steady-state Kinetics Assay—Steady-state kinetic parameters for nucleotide insertion opposite dG, rG, 8-oxo-rG, or 8-oxo-dG and chain extension from the 3′ terminus were determined at 25 °C, using varying amounts of single dNTPs as described previously (33). For nucleotide insertion, the reaction mixture contained 38-mer template (750 fmol) primed with Alexa 546-labeled 12-mer (500 fmol; 5′-AGAGGAAAGAAG). To measure chain extension, the reaction mixture contained 38-mer template (750 fmol) primed with an Alexa 546-labeled 13-mer (500 fmol; 5′-AGAGGAAAGAAGN, where N was C, A, G, or T). Enzyme concentrations and reaction times were chosen so that product inhibition and substrate depletion did not influence the observed rate. The reaction samples were subjected to 20% denaturing PAGE (30 × 40 × 0.05 cm). The rate of incorporation was plotted against dNTP concentrations, and the apparent Michaelis-Menten constants, K_m, and V_{max} values were determined by the Enzyme Kinetics Module 1.1 of SigmaPlot 2001 software version 7.101 (SPSS, Inc). The k_{cat} value was calculated by dividing the V_{max} by the enzyme concentration. F_{ins} and F_{ext} values were determined relative to the dC:dG base pair according to the following equation: $F = (k_{cat}/K_m)_{[\text{wrong pair}]}/(k_{cat}/K_m)_{[\text{correct pair = dC:dG}]}$ (53, 54).

DNA Glycosylase Assay—DNA substrates were constructed by annealing 5′-6-FAM-labeled 38-mer oligonucleotides (5′-CATGCTGATGAATTCCTTC*X*CTTCTTTCCTCTCCCTTT, where *X* indicates rG, 8-oxo-rG, or 8-oxo-dG) to their complementary strand. The reaction mixture in a final volume of 10 μl contained 200 nM DNA substrate, 50 mM Hepes (pH 7.5), 20 mM KCl, 5 mM $MgCl_2$, 0.5 mM EDTA, and 0.1% BSA. The reactions were started with the addition of OGG1 (100 nM) with or without APE1 (40 nM), and incubated at 37 °C for 30 min, and then stopped with an equal volume of dye containing 95% formamide, 20 mM EDTA, 0.02% bromphenol blue, and 0.02% xylene cyanol. The reaction products were separated by PAGE and analyzed as described above.

RNase Assay—5′-6-FAM-labeled DNA substrates containing rG and 8-oxo-rG were constructed as described above. The reaction mixture in a final volume of 10 μl contained 200 nM DNA substrate and 1× ThermoPol reaction buffer (20 mM Tris-HCl (pH 8.8), 10 mM $(NH_4)_2SO_4$, 10 mM KCl, 2 mM $MgSO_4$, 0.1% Triton X-100). Reactions were initiated by the addition of RNase H2 (0.5, 1.0, or 1.5 units) or the enzyme mixture including both RNase H2 (0.5, 1.0, or 1.5 units) and OGG1 (750 nM) that was preheated at 37 °C for 5 min. Both reaction mixtures were then incubated at 37 °C for 60 min, and stopped with an equal volume of 95% formamide dye. The reaction samples were subjected to PAGE and analyzed as described above.

Gel Mobility Shift Assay—The 5′-6-FAM-labeled DNA substrates containing 8-oxo-rG and 8-oxo-dG were prepared as described above. The reaction mixture in a final volume of 15 μl contained 50 nM DNA substrate, 50 mM Hepes (pH 7.5), 20 mM KCl, 5 mM $MgCl_2$, 0.5 mM EDTA, 0.1% BSA, and varying amounts of OGG1. The reaction mixtures were incubated on ice for 15 min and immediately separated in a non-denaturing 10% polyacrylamide gel (acrylamide:bis-acrylamide = 37.5:1). To help maintain integrity of bound complexes during PAGE, the gel was run in the cold room. The gel was analyzed using Typhoon PhosphorImager (GE Healthcare) as described above.

Statistical Analysis—The statistical significance was evaluated using Scheffe's test or Tukey's honest significant difference test.

Author Contributions—A. S. designed the research; A. S., M. Ç., Y. R., and M. Y. set up the experiments; A. S., M. Ç., Y. R., W. A. B., S. H. W., M. H., and M. Y. discussed the study; A. S., M. Ç., and Y. R. performed the research and analyzed data; A. S. and M. Ç. wrote the paper; W. A. B., S. H. W., T. N., M. H., and M. Y. provided the research direction; M. Y. and M. H. commented on the results and the manuscript at all stages; W. A. B., S. H. W., T. N., M. H., and M. Y. revised the paper; all authors approved the final version of the manuscript.

Acknowledgments—We thank Dr. Masashi Hyuga (National Institute of Health Sciences) for allowing us to use the Typhoon PhosphorImager. We also thank Enago (www.enago.jp) for the English-language review.

References

1. Nick McElhinny, S. A., Watts, B. E., Kumar, D., Watt, D. L., Lundström, E. B., Burgers, P. M., Johansson, E., Chabes, A., and Kunkel, T. A. (2010)

Abundant ribonucleotide incorporation into DNA by yeast replicative polymerases. *Proc. Natl. Acad. Sci. U.S.A.* **107,** 4949–4954
2. Traut, T. W. (1994) Physiological concentrations of purines and pyrimidines. *Mol. Cell. Biochem.* **140,** 1–22
3. Reijns, M. A., Rabe, B., Rigby, R. E., Mill, P., Astell, K. R., Lettice, L. A., Boyle, S., Leitch, A., Keighren, M., Kilanowski, F., Devenney, P. S., Sexton, D., Grimes, G., Holt, I. J., Hill, R. E., *et al.* (2012) Enzymatic removal of ribonucleotides from DNA is essential for mammalian genome integrity and development. *Cell* **149,** 1008–1022
4. Sparks, J. L., Chon, H., Cerritelli, S. M., Kunkel, T. A., Johansson, E., Crouch, R. J., and Burgers, P. M. (2012) RNase H2-initiated ribonucleotide excision repair. *Mol. Cell* **47,** 980–986
5. Williams, J. S., Smith, D. J., Marjavaara, L., Lujan, S. A., Chabes, A., and Kunkel, T. A. (2013) Topoisomerase 1-mediated removal of ribonucleotides from nascent leading-strand DNA. *Mol. Cell* **49,** 1010–1015
6. Nick McElhinny, S. A., Kumar, D., Clark, A. B., Watt, D. L., Watts, B. E., Lundström, E. B., Johansson, E., Chabes, A., and Kunkel, T. A. (2010) Genome instability due to ribonucleotide incorporation into DNA. *Nat. Chem. Biol.* **6,** 774–781
7. Kim, N., Huang, S. N., Williams, J. S., Li, Y. C., Clark, A. B., Cho, J. E., Kunkel, T. A., Pommier, Y., and Jinks-Robertson, S. (2011) Mutagenic processing of ribonucleotides in DNA by yeast topoisomerase I. *Science* **332,** 1561–1564
8. Crow, Y. J., Leitch, A., Hayward, B. E., Garner, A., Parmar, R., Griffith, E., Ali, M., Semple, C., Aicardi, J., Babul-Hirji, R., Baumann, C., Baxter, P., Bertini, E., Chandler, K. E., *et al.* (2006) Mutations in genes encoding ribonuclease H2 subunits cause Aicardi-Goutieres syndrome and mimic congenital viral brain infection. *Nat. Genet.* **38,** 910–916
9. Lim, Y. W., Sanz, L. A., Xu, X., Hartono, S. R., and Chedin, F. (2015) Genome-wide DNA hypomethylation and RNA:DNA hybrid accumulation in Aicardi-Goutieres syndrome. *eLife* **4,** 10.7554/eLife.08007
10. Tsuzuki, T., Nakatsu, Y., and Nakabeppu, Y. (2007) Significance of error-avoiding mechanisms for oxidative DNA damage in carcinogenesis. *Cancer Sci.* **98,** 465–470
11. Nakabeppu, Y., Sakumi, K., Sakamoto, K., Tsuchimoto, D., Tsuzuki, T., and Nakatsu, Y. (2006) Mutagenesis and carcinogenesis caused by the oxidation of nucleic acids. *Biol. Chem.* **387,** 373–379
12. Maki, H., and Sekiguchi, M. (1992) MutT protein specifically hydrolyses a potent mutagenic substrate for DNA synthesis. *Nature* **355,** 273–275
13. Rosenquist, T. A., Zharkov, D. O., and Grollman, A. P. (1997) Cloning and characterization of a mammalian 8-oxoguanine DNA glycosylase. *Proc. Natl. Acad. Sci. U.S.A.* **94,** 7429–7434
14. Michaels, M. L., Tchou, J., Grollman, A. P., and Miller, J. H. (1992) A repair system for 8-oxo-7,8-dihydrodeoxyguanine. *Biochemistry* **31,** 10964–10968
15. Xie, Y., Yang, H., Cunanan, C., Okamoto, K., Shibata, D., Pan, J., Barnes, D. E., Lindahl, T., McIlhatton, M., Fishel, R., and Miller, J. H. (2004) Deficiencies in mouse Myh and Ogg1 result in tumor predisposition and G to T mutations in codon 12 of the K-ras oncogene in lung tumors. *Cancer Res.* **64,** 3096–3102
16. Kamiya, H., Suzuki, A., Kawai, K., Kasai, H., and Harashima, H. (2007) Effects of 8-hydroxy-GTP and 2-hydroxy-ATP on *in vitro* transcription. *Free Radic. Biol. Med.* **43,** 837–843
17. Calabretta, A., Küpfer, P. A., and Leumann, C. J. (2015) The effect of RNA base lesions on mRNA translation. *Nucleic Acids Res.* **43,** 4713–4720
18. Sastre-Moreno, G., Sánchez, A., Esteban, V., and Blanco, L. (2014) ATP insertion opposite 8-oxo-deoxyguanosine by Pol4 mediates error-free tolerance in *Schizosaccharomyces pombe*. *Nucleic Acids Res.* **42,** 9821–9837
19. Ordonez, H., and Shuman, S. (2014) *Mycobacterium smegmatis* DinB2 misincorporates deoxyribonucleotides and ribonucleotides during templated synthesis and lesion bypass. *Nucleic Acids Res.* **42,** 12722–12734
20. Cilli, P., Minoprio, A., Bossa, C., Bignami, M., and Mazzei, F. (2015) Formation and repair of mismatches containing ribonucleotides and oxidized bases at repeated DNA sequences. *J. Biol. Chem.* **290,** 26259–26269
21. Zhang, Y., Yuan, F., Wu, X., Wang, M., Rechkoblit, O., Taylor, J. S., Geacintov, N. E., and Wang, Z. (2000) Error-free and error-prone lesion bypass by human DNA polymerase κ *in vitro*. *Nucleic Acids Res.* **28,** 4138–4146
22. Zhang, Y., Wu, X., Guo, D., Rechkoblit, O., and Wang, Z. (2002) Activities of human DNA polymerase kappa in response to the major benzo[*a*]pyrene DNA adduct: error-free lesion bypass and extension synthesis from opposite the lesion. *DNA Repair* **1,** 559–569
23. Sassa, A., Niimi, N., Fujimoto, H., Katafuchi, A., Grúz, P., Yasui, M., Gupta, R. C., Johnson, F., Ohta, T., and Nohmi, T. (2011) Phenylalanine 171 is a molecular brake for translesion synthesis across benzo[*a*]pyrene-guanine adducts by human DNA polymerase kappa. *Mutat. Res.* **718,** 10–17
24. Johnson, R. E., Prakash, S., and Prakash, L. (1999) Efficient bypass of a thymine-thymine dimer by yeast DNA polymerase, Polη. *Science* **283,** 1001–1004
25. Masutani, C., Kusumoto, R., Yamada, A., Dohmae, N., Yokoi, M., Yuasa, M., Araki, M., Iwai, S., Takio, K., and Hanaoka, F. (1999) The XPV (xeroderma pigmentosum variant) gene encodes human DNA polymerase η. *Nature* **399,** 700–704
26. Kamiya, H., and Kurokawa, M. (2012) Mutagenic bypass of 8-oxo-7,8-dihydroguanine (8-hydroxyguanine) by DNA polymerase κ in human cells. *Chem. Res. Toxicol.* **25,** 1771–1776
27. Rodriguez, G. P., Song, J. B., and Crouse, G. F. (2013) *In vivo* bypass of 8-oxodG. *PLoS Genet.* **9,** e1003682
28. Clausen, A. R., Murray, M. S., Passer, A. R., Pedersen, L. C., and Kunkel, T. A. (2013) Structure-function analysis of ribonucleotide bypass by B family DNA replicases. *Proc. Natl. Acad. Sci. U.S.A.* **110,** 16802–16807
29. Lazzaro, F., Novarina, D., Amara, F., Watt, D. L., Stone, J. E., Costanzo, V., Burgers, P. M., Kunkel, T. A., Plevani, P., and Muzi-Falconi, M. (2012) RNase H and postreplication repair protect cells from ribonucleotides incorporated in DNA. *Mol. Cell* **45,** 99–110
30. Haracska, L., Yu, S. L., Johnson, R. E., Prakash, L., and Prakash, S. (2000) Efficient and accurate replication in the presence of 7,8-dihydro-8-oxoguanine by DNA polymerase η. *Nat. Genet.* **25,** 458–461
31. Patra, A., Nagy, L. D., Zhang, Q., Su, Y., Müller, L., Guengerich, F. P., and Egli, M. (2014) Kinetics, structure, and mechanism of 8-oxo-7,8-dihydro-2′-deoxyguanosine bypass by human DNA polymerase η. *J. Biol. Chem.* **289,** 16867–16882
32. Sassa, A., Ohta, T., Nohmi, T., Honma, M., and Yasui, M. (2011) Mutational specificities of brominated DNA adducts catalyzed by human DNA polymerases. *J. Mol. Biol.* **406,** 679–686
33. Yasui, M., Suenaga, E., Koyama, N., Masutani, C., Hanaoka, F., Gruz, P., Shibutani, S., Nohmi, T., Hayashi, M., and Honma, M. (2008) Miscoding properties of 2′-deoxyinosine, a nitric oxide-derived DNA Adduct, during translesion synthesis catalyzed by human DNA polymerases. *J. Mol. Biol.* **377,** 1015–1023
34. Lu, R., Nash, H. M., and Verdine, G. L. (1997) A mammalian DNA repair enzyme that excises oxidatively damaged guanines maps to a locus frequently lost in lung cancer. *Curr. Biol.* **7,** 397–407
35. Tominaga, Y., Ushijima, Y., Tsuchimoto, D., Mishima, M., Shirakawa, M., Hirano, S., Sakumi, K., and Nakabeppu, Y. (2004) MUTYH prevents OGG1 or APEX1 from inappropriately processing its substrate or reaction product with its C-terminal domain. *Nucleic Acids Res.* **32,** 3198–3211
36. Sassa, A., Çalayan, M., Dyrkheeva, N. S., Beard, W. A., and Wilson, S. H. (2014) Base excision repair of tandem modifications in a methylated CpG dinucleotide. *J. Biol. Chem.* **289,** 13996–14008
37. Biertümpfel, C., Zhao, Y., Kondo, Y., Ramón-Maiques, S., Gregory, M., Lee, J. Y., Masutani, C., Lehmann, A. R., Hanaoka, F., and Yang, W. (2010) Structure and mechanism of human DNA polymerase η. *Nature* **465,** 1044–1048
38. Lone, S., Townson, S. A., Uljon, S. N., Johnson, R. E., Brahma, A., Nair, D. T., Prakash, S., Prakash, L., and Aggarwal, A. K. (2007) Human DNA polymerase κ encircles DNA: implications for mismatch extension and lesion bypass. *Mol. Cell* **25,** 601–614
39. Vasquez-Del Carpio, R., Silverstein, T. D., Lone, S., Swan, M. K., Choudhury, J. R., Johnson, R. E., Prakash, S., Prakash, L., and Aggarwal, A. K. (2009) Structure of human DNA polymerase κ inserting dATP opposite an 8-OxoG DNA lesion. *PLoS ONE* **4,** e5766
40. Uesugi, S., and Ikehara, M. (1977) Carbon-13 magnetic resonance spectra of 8-substituted purine nucleosides: characteristic shifts for the syn conformation. *J. Am. Chem. Soc.* **99,** 3250–3253
41. Krahn, J. M., Beard, W. A., Miller, H., Grollman, A. P., and Wilson, S. H. (2003) Structure of DNA polymerase β with the mutagenic DNA lesion 8-oxodeoxyguanine reveals structural insights into its coding potential. *Structure* **11,** 121–127

42. DeRose, E. F., Perera, L., Murray, M. S., Kunkel, T. A., and London, R. E. (2012) Solution structure of the Dickerson DNA dodecamer containing a single ribonucleotide. *Biochemistry* **51,** 2407–2416
43. Bruner, S. D., Norman, D. P., and Verdine, G. L. (2000) Structural basis for recognition and repair of the endogenous mutagen 8-oxoguanine in DNA. *Nature* **403,** 859 – 866
44. Küpfer, P. A., and Leumann, C. J. (2007) The chemical stability of abasic RNA compared to abasic DNA. *Nucleic Acids Res.* **35,** 58 – 68
45. Vaisman, A., McDonald, J. P., Huston, D., Kuban, W., Liu, L., Van Houten, B., and Woodgate, R. (2013) Removal of misincorporated ribonucleotides from prokaryotic genomes: an unexpected role for nucleotide excision repair. *PLoS Genet.* **9,** e1003878
46. Guo, J., Hanawalt, P. C., and Spivak, G. (2013) Comet-FISH with strand-specific probes reveals transcription-coupled repair of 8-oxo-guanine in human cells. *Nucleic Acids Res.* **41,** 7700 –7712
47. Sassa, A., Kamoshita, N., Kanemaru, Y., Honma, M., and Yasui, M. (2015) *Xeroderma pigmentosum* group A suppresses mutagenesis caused by clustered oxidative DNA adducts in the human genome. *PLoS ONE* **10,** e0142218
48. Reardon, J. T., Bessho, T., Kung, H. C., Bolton, P. H., and Sancar, A. (1997) *In vitro* repair of oxidative DNA damage by human nucleotide excision repair system: possible explanation for neurodegeneration in xeroderma pigmentosum patients. *Proc. Natl. Acad. Sci. U.S.A.* **94,** 9463–9468
49. Niimi, N., Sassa, A., Katafuchi, A., Grúz, P., Fujimoto, H., Bonala, R. R., Johnson, F., Ohta, T., and Nohmi, T. (2009) The steric gate amino acid tyrosine 112 is required for efficient mismatched-primer extension by human DNA polymerase κ. *Biochemistry* **48,** 4239 – 4246
50. Sassa, A., Beard, W. A., Shock, D. D., and Wilson, S. H. (2013) Steady-state, pre-steady-state, and single-turnover kinetic measurement for DNA glycosylase activity. *J. Vis. Exp.* **19,** e50695
51. Strauss, P. R., Beard, W. A., Patterson, T. A., and Wilson, S. H. (1997) Substrate binding by human apurinic/apyrimidinic endonuclease indicates a Briggs-Haldane mechanism. *J. Biol. Chem.* **272,** 1302–1307
52. Shibutani, S. (1993) Quantitation of base substitutions and deletions induced by chemical mutagens during DNA synthesis *in vitro*. *Chem. Res. Toxicol.* **6,** 625– 629
53. Mendelman, L. V., Petruska, J., and Goodman, M. F. (1990) Base mispair extension kinetics: comparison of DNA polymerase α and reverse transcriptase. *J. Biol. Chem.* **265,** 2338 –2346
54. Mendelman, L. V., Boosalis, M. S., Petruska, J., and Goodman, M. F. (1989) Nearest neighbor influences on DNA polymerase insertion fidelity. *J. Biol. Chem.* **264,** 14415–14423